Peer-reviewed version available at *Geosciences* **2018**, *8*, 309; doi:10.3390/geosciences8090309

Article

Removal of barium, cobalt, strontium and zinc from solution by natural and synthetic allophane adsorbents

Andre Baldermann [1,*], Andrea Cäcilia Grießbacher [1], Claudia Baldermann [2], Bettina Purgstaller [1], Ilse Letofsky-Papst [3], Stephan Kaufhold [4] and Martin Dietzel [1]

[1] Institute of Applied Geosciences, Graz University of Technology, Rechbauerstraße 12, 8010 Graz, Austria; baldermann@tugraz.at; andrea.griessbacher@student.tugraz.at; bettina.purgstaller@tugraz.at; martin.dietzel@tugraz.at

[2] Institute of Technology and Testing of Building Materials, Graz University of Technology, Inffeldgasse 24, 8010 Graz, Austria; claudia.baldermann@tugraz.at

[3] Institute for Electron Microscopy and Nanoanalysis and Center for Electron Microscopy, Graz University of Technology, Steyrergasse 17, 8010 Graz, Austria; ilse.papst@felmi-zfe.at

[4] BGR, Bundesanstalt für Geowissenschaften und Rohstoffe, Geozentrum Hannover, Stilleweg 2, 30655 Hannover, Germany; stephan.kaufhold@bgr.de

* Correspondence: baldermann@tugraz.at; Tel.: +43-(0)316-873-6850

Abstract: The capacity and the mechanism of the adsorption of aqueous barium (Ba), cobalt (Co), strontium (Sr) and zinc (Zn) by Ecuadorian (NatAllo) and synthetic (SynAllo-1 and SynAllo-2) allophanes were studied as a function of contact time, pH and metal ion concentration using kinetic and equilibrium experiments. The mineralogy, nano-structure and chemical composition of the allophanes were characterized by X-ray diffraction, Fourier transform infrared spectroscopy, transmission electron microscopy and specific surface area analyses. The evolution of adsorption fitted to a pseudo-first-order reaction kinetics, where equilibrium between aqueous metal ions and allophane was reached within < 10 min. The metal ion removal efficiencies varied from 0.7 to 99.7 % at pH 4.0 to 8.5. At equilibrium, the adsorption behavior is better described by the Langmuir model than by the Dubinin-Radushkevich model, yielding sorption capacities of 10.6, 17.2 and 38.6 mg/g for Ba^{2+}, 12.4, 19.3 and 29.0 mg/g for $HCoO_2^-$, 7.2, 15.9 and 34.4 mg/g for Sr^{2+} and 20.9, 26.9 and 36.9 mg/g for Zn^{2+}, respectively, by NatAllo, SynAllo-2 and SynAllo-1. The uptake mechanism is based on a physical adsorption process. Allophane holds great potential to remove aqueous metal ions and could be used instead of zeolites, montmorillonite, carbonates and phosphates for wastewater treatment.

Keywords: allophane; adsorption; precipitation; interface processes; environment; heavy metals; nano-structure; short-range order aluminosilicate; wastewater treatment; aqueous geochemistry

1. Introduction

Pollution of groundwater and drinking water by heavy metals is increasingly becoming a major environmental issue worldwide. Heavy metals are typically released by the weathering of rocks and minerals and from a wide range of human activities such as agriculture, energy production, manufacturing, transportation, mining and waste disposal [1]. They often cause deleterious effects on aquatic life and to the terrestrial environment [2,3]. Contamination of surface water and groundwater with toxic and/or cancerogenic heavy metals and its subsequent use as a source of drinking water without previous treatment is a major threat to human health [4–6]. To date, ~40 % of the world's population suffer from water scarcity and lack access to unpolluted water or basic sanitation [7]. Consequently, there is a high demand for the development of new techniques and materials for wastewater treatment. In recent times, different techniques for the removal of aqueous metal ions have been developed and are routinely used in practice such as adsorption, precipitation,

ion exchange, flocculation, sedimentation, membrane filtration and electrochemical methods [8,9]. Contemporarily, natural and synthetic macro-, micro- and nano-adsorbents and nano-composites have been manufactured and are now successfully applied in water processing plants.

Generally, a small particle size (< 10-100 nm), a large specific surface area (> 10 m^2/g) and the presence of surface functional groups (i.e. ≡Al-OH° and ≡Si-OH°) in adsorbents are favorable to ensure a desired adsorption rate and appropriate metal ion removal efficiency [10,11]. Recently, agricultural and industrial waste products, activated carbon nanotubes, cellulose, carbonates, Fe- and Al-oxyhydroxides, zeolites, phosphates and clay minerals are used in the remediation of water that is severely polluted with persistent and hazardous components such as heavy metal ions, dyes, antibiotics, biocide compounds and other organic chemicals [12–16]. The use of clay minerals for wastewater treatment can be advantageous over other sorbents due to their worldwide occurrence, low mining and processing costs and outstanding physicochemical and surface properties, making clayey materials suitable for selective ion exchange, adsorption and catalyst uses [1,17,18].

The short-range order aluminosilicate allophane ($1\text{-}2SiO_2 \cdot Al_2O_3 \cdot 5\text{-}6H_2O$) is a naturally occurring clay mineral, which is distributed in volcanic ash layers and in soil profiles worldwide. Allophane has a 3.5 to 5.0 nm sized hollow spherical structure with 0.3-0.5 nm sized defect sites (so-called perforations or pore regions) on its surface [19–21]. Allophane "nanoballs" are characterized by a high surface area (> 300 m^2/g). They are well-known to adsorb appreciable amounts of ionic or polar pollutants due to an amphoteric ligand exchange capacity [17,22,23]. To date, however, the sorption properties of allophane have not been effectively utilized in the remediation of wastewater. Basic studies are needed to explore the potential of allophane for water treatment. Therefore, in this study we investigated the adsorption kinetics and the mechanisms of the uptake of aqueous Ba, Co, Sr and Zn species by Ecuadorian allophane and two synthetic allophanes at 25 °C as a function of contact time, pH and initial metal ion concentration. The metal ion-specific adsorption rates and the removal efficiencies of both natural and synthetic allophanes are presented and discussed in relation to the potential use of allophane in water processing technologies.

2. Materials, Experimental and Methods

2.1. Materials

Allophane-rich soil material from the "allophane facies" of the Santo Domingo de los Colorados deposit in Ecuador ("NatAllo") and two synthetic allophanes ("SynAllo-1" and "SynAllo-2") were used for the adsorption studies. NatAllo was used as received without further purification (sample 4-7; [24]). SynAllo-1 and SynAllo-2 were precipitated by modifying the method of Wada et al. [25]. Briefly, 1.0 L of a stock solution containing 100 mM of $Si(OH)_4$ ($Na_2SiO_3 \cdot 2H_2O$ from Roth) was mixed with anhydrous $AlCl_3$ (SynAllo-1) or $Al(NO_3)_3 \cdot 9H_2O$ salts (SynAllo-2) from Roth to obtain an initial aqueous molar Al/Si ratio of 1. The experimental solution was adjusted to pH 6.0 ± 0.1 using a 0.1 M NaOH solution and mingled at 150 rpm for 2 h using a magnetic stirrer at 25 °C. Subsequently, the experimental solution was aged at 80 °C in a compartment drier within the sealed high-density polyethylene batch reactor. After 48 h the experiments were terminated. The solids were separated by a 0.45 μm filter (Sartorius, cellulose acetate) using a suction filtration unit, washed with deionized water to remove electrolytes and dried at 40 °C.

For the adsorption experiments, individual stock solutions of Ba(II), Co(II), Sr(II) and Zn(II) were prepared by the dissolution of analytical grade chemicals ($BaCl_2 \cdot 2H_2O$, $CoCl_2 \cdot 6H_2O$ and NaCl from Roth; $SrCl_2 \cdot 6H_2O$ and $ZnCl_2$ from Merck) in deionized water (Milli-Q Plus UV, Millipore, 18.2 MΩ at 25 °C). Each stock solution contained 230 mg/L (10 mM) of NaCl as background electrolyte.

2.2. Adsorption experiments

Batch experiments were carried out to evaluate the effect of contact time, pH and initial metal ion concentration on the adsorption capacity and on the rate of aqueous Ba, Co, Sr and Zn removal by natural and synthetic allophanes at 25 °C. The effect of contact time on the adsorption behavior of aqueous metal ions by allophane was studied in a first set of experiments conducted at a constant pH of either 8.5 or 5.5, each ± 0.1 pH units. These experiments were carried out in 1.5 L high-density polyethylene reactors containing 1000 mL of the adsorbate (10 mg/L) and 2.0 g of the adsorbent. Immediately after placing the allophane in the reactor, the experimental solutions were adjusted to pH 8.5 or 5.5 with 0.1 M NaOH or 0.05 M HCl solutions. Fluid sampling (~1 mL) started instantly after the adjustment of the target pH value. Samples were taken after 10 s, 30 s, 1 min, 3 min, 5 min, 10 min, 1 h and 1 day using a syringe (B.Braun, Omnifix^R Solo), filtered via 0.45 µm cellulose acetate filters (Sartorius) and acidified using $\mathbf{HNO_3}$ of suprapure grade (Roth, ROTIPURAN^R).

The effect of pH on the uptake of aqueous metal ions by natural and synthetic allophanes was studied in a second set of batch experiments in the pH range from 8.5 to 4.0. The pH of the allophane suspensions was allowed to drift to a constant value (pH ~7-8), which required less than 1 h. The suspensions were then adjusted to pH 8.5 ± 0.1 with 0.1 M NaOH solutions. All suspensions were stirred at 150 rpm for 2 h to ensure both the complete surface rehydration of the allophanes and the establishment of adsorption equilibrium between adsorbent and adsorbate. Afterwards, droplets of a 0.05 M HCl solution were added to the experimental solution to induce a pH decrease from 8.5 ± 0.1 to 4.0 ± 0.2. The stepwise addition of the acid and fluid sampling (~1 mL á ~0.5 pH units) caused in all experiments less than ~1.3 % change of the initial fluid volume and therefore no corrections for the metal ion concentration in solution were made. All experiments were of short duration (< 2 h) in order to minimize changes in the surface area and surface properties of the allophanes.

In a third set of experiments, the effect of metal ion concentration on the adsorption behavior of allophanes was investigated at pH 8.5 ± 0.1 for 2 h using 0.1 g of the adsorbent and 50 mL of solution containing Ba, Co, Sr and Zn in different concentrations (1, 10, 20, 50 and 100 mg/L). The suspensions were prepared in analogy to those from the second set of experiments. The fluid sampling strategy was identical to the procedure described above.

The amount of metal ions adsorbed on the allophanes (q_e: mg/g) was calculated using Eq. 1:

$$\boldsymbol{q_e = \frac{(C_0 - C_e)}{m} \times V} \quad (1)$$

where C_o and C_e are the initial and the equilibrium concentrations of the adsorbate (mg/L), m is the dry mass of the adsorbent (g) and V is the volume of the adsorbate solution (L).

The adsorption efficiency (%removal) is expressed by the percentage of removed adsorbate at equilibrium, according to Eq. 2:

$$\boldsymbol{\%removal = \frac{(C_0 - C_e)}{C_0} \times 100} \quad (2)$$

2.3. Analytical methods

2.3.1. Fluid-phase characterization

The solution pH was measured at 25 °C with a SenTix 41 glass electrode connected to a WTW Multi 350i pH-meter, which was calibrated against NIST buffer standard solutions at pH 4.01, 7.00 and 10.00 (analytical error: ± 0.05 pH units).

The total concentrations of aqueous Al, Ba, Co, Na, Si, Sr and Zn were analyzed in acidified samples by inductively coupled plasma optical emission spectroscopy (ICP-OES) using a Perkin Elmer Optima 8300. The analytical precision (2σ, 3 replicates) of the ICP-OES measurements was determined as ± 2 % for Ba, Na, Si and Sr analyses and ± 3 % for Al, Co and Zn analyses, respectively, relative to the NIST 1640a and SPS-SW2 Batch 130 standards.

The aqueous speciation of the solutions and the saturation degrees of the metal oxyhydroxides of Ba(II), Co(II), Sr(II) and Zn(II) were calculated using the PHREEQC software in combination with

its implemented Lawrence Livermore National Laboratory (LLNL) database at the experimental pH and temperature.

2.3.2. Solid-phase characterization

The mineralogy of the adsorbent materials was examined by X-ray diffraction (XRD) using a PANalytical X'Pert PRO diffractometer (Co-Kα radiation) operated at 40 kV and 40 mA and outfitted with a spinner stage, 0.5° antiscattering slit, 1° divergence slit, primary and secondary soller and a high-speed Scientific X'Celerator detector. The specimens were examined in the range 4-85° 2θ with a step size of 0.008° 2θ and a counting time of 40 s per step. Mineral quantification was carried out by Rietveld refinement of the XRD patterns using the PANanalytical X`Pert Highscore Plus software package (version 2.2e) and a pdf-4 database.

Attenuated total reflectance Fourier transform infrared (ATR-FTIR) spectroscopy data were obtained for further characterization of the allophanes by a PerkinElmer Frontier FTIR. Mid-infrared (MIR) spectra were recorded in the range from 4000-650 cm^{-1} at a resolution of 2 cm^{-1}.

The specific surface area of the natural and synthetic allophanes before and after the adsorption experiments was analyzed on dried (100 °C for 24 h) aliquots by the multi-point adsorption BET method using a Micrometrics FlowSorb II2300 and a He(69.8)-N_2(30.2) mixture as the carrier gas. The estimated analytical uncertainty is ± 10 %.

The particle shape, the nano-structure and the geochemical composition of the allophanes were analyzed by transmission electron microscopy (TEM) on a FEI Tecnai F20 operated at an accelerating voltage of 200 kV. This instrument is fitted with a single-crystal LaB_6 Schottky Field Emitter, a Gatan imaging filter and an UltraScan CCD camera for high-resolution imaging and selected area electron diffraction (SAED), and an EDAX Saphire Si(Li) detector for energy-dispersive X-ray spectroscopy (EDX) analysis. The TEM-EDX spectra were acquired using a counting time of 30 s to reduce element migration and element loss. The accuracy of the EDX results was verified by replicate measurements performed on a suite of phyllosilicate standards [26–28]. The analytical error was determined to be ± 2 at.% for Si and Al analyses.

3. Results and Discussion

3.1. Mineralogical characterization of allophane adsorbents

XRD analysis confirmed the dominance of allophane in NatAllo (~78 wt.%; [24,29]) which also contains minor quantities (each < 5 wt.%) of quartz, cristobalite, feldspar (albite and orthoclase), hornblende, halloysite, gibbsite and goethite (Fig. 1). The XRD patterns of SynAllo-1 and SynAllo-2 exhibited two broad peaks centered at ~3.4 Å and ~2.3 Å, which is typical for short-range ordered aluminosilicates such as allophane. No indication for the formation of amorphous silica or discrete Al-O-OH phases such as boehmite and gibbsite was found in the synthetic precipitates, implying that SynAllo-1 and SynAllo-2 solely consist of allophane. However, in these samples the presence of traces of amorphous Al-hydroxides cannot be excluded. The XRD patterns of natural and synthetic allophanes after the adsorption experiments (patterns are not shown) do not reveal the formation of Ba(II), Co(II), Sr(II) and Zn(II) oxyhydroxides).

The MIR spectra of the allophanes before and after the adsorption experiments displayed very similar profiles. Figure 2 presents IR spectra of unreacted allophane and with sorbed Zn^{2+} ions (for experiments with aqueous Ba, Co and Sr similar spectra were obtained, but are not shown). The IR bands of the metal ions adsorbed could not be resolved, because the adsorbate concentration is low relative to those of the adsorbent. The presence of halloysite in NatAllo is indicated by two IR bands in the OH-stretching region (3600-3700 cm^{-1}). In addition, gibbsite and quartz were identified in this sample, which matches with the XRD results. The main lattice vibration bands of the allophanes are located between 1000–980cm^{-1} and at 870 cm^{-1} due to Si-O-(Si) or Si-O-(Al) vibrations and Si-OH groups [19,30,31]. The IR spectra of SynAllo-1 and SynAllo-2 are similar to those reported for natural allophane, which shows that proto-imogolite allophane or imogolite structures did not form under the given experimental conditions [19,25,32].

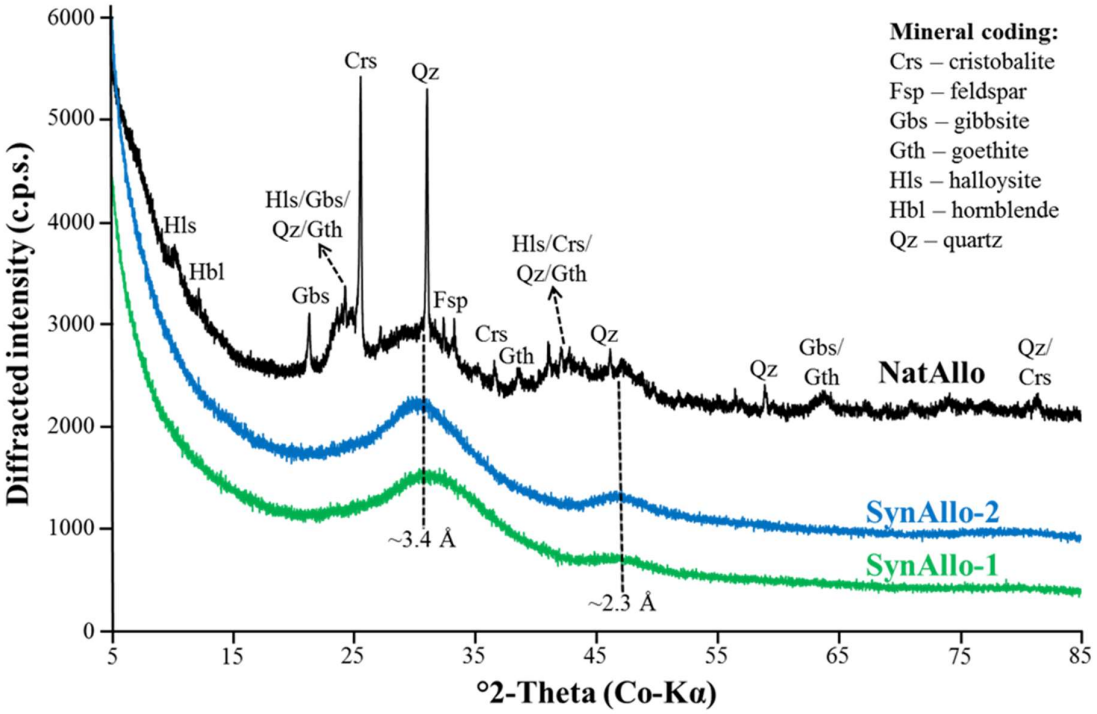

Figure 1. XRD patterns of Ecuadorian allophane (NatAllo) and synthetic allophanes (SynAllo-1 and SynAllo-2) used as adsorbents. Data obtained after the adsorption experiments are not shown since all samples displayed similar patterns. Peaks at ~3.4 Å and ~2.3 Å correspond to allophane.

3.2. Structural and chemical characterization of allophane adsorbents

Representative TEM images of allophane nano-particles are shown in Figure 3. The allophane particles from NatAllo, SynAllo-1 and SynAllo-2 are 5 ± 2 nm, 8 ± 3 nm and 10 ± 5 nm, on average, in largest dimension and have an aspect ratio equal to 1. The SAED patterns of natural and synthetic allophanes display weak diffraction rings or smeared Bragg patterns (Fig. 3E-F), which is typical for short-range ordered aluminosilicates, i.e. allophane. Such allophane structures are often described as ring-shaped, hollow spherules or allophane nano-balls [19,31].

The specific surface areas were determined are 294 m^2/g for NatAllo, 358 m^2/g for SynAllo-1 and 370 m^2/g for SynAllo-2, respectively. These values are in the range of N_2-BET values previously reported for natural allophanes (~200-400 m^2/g) and synthetic allophanes (~250-900 m^2/g) [10,29,33]. Noteworthy, the BET values obtained before and after the adsorption experiments were identical to within the analytical precision of the BET analyses, which indicates that changes in the surface area and surface properties of the adsorbents are negligible throughout the experiments.

Allophanes are classified by their atomic Al/Si ratio, with Al-rich proto-imogolite allophane or imogolite-like allophanes (Al/Si = 2) and Si-rich halloysite-like or pumice allophanes (Al/Si = 1) as the members [19]. TEM-EDX analysis of cloud-like particle aggregates of NatAllo yielded an averaged atomic Al/Si ratio of 1.3 ± 0.2 (Fig. 3d), corroborating the atomic Al/Si ratio of 1.3–1.4 for Ecuadorian allophane previously reported in Kaufhold et al. [24]. Such allophanes are very often referred to as "stream deposit allophanes" or "silica springs allophane", according to Parfitt [19]. Minor amounts of Fe in NatAllo (Fig. 3d) most likely belong to fine-grained goethite particles, being dispersed in the allophane aggregates. The atomic Al/Si ratio of the synthetic allophanes was determined as 1.0 ± 0.1 (Fig. 3d), which is close to the Si-rich member.

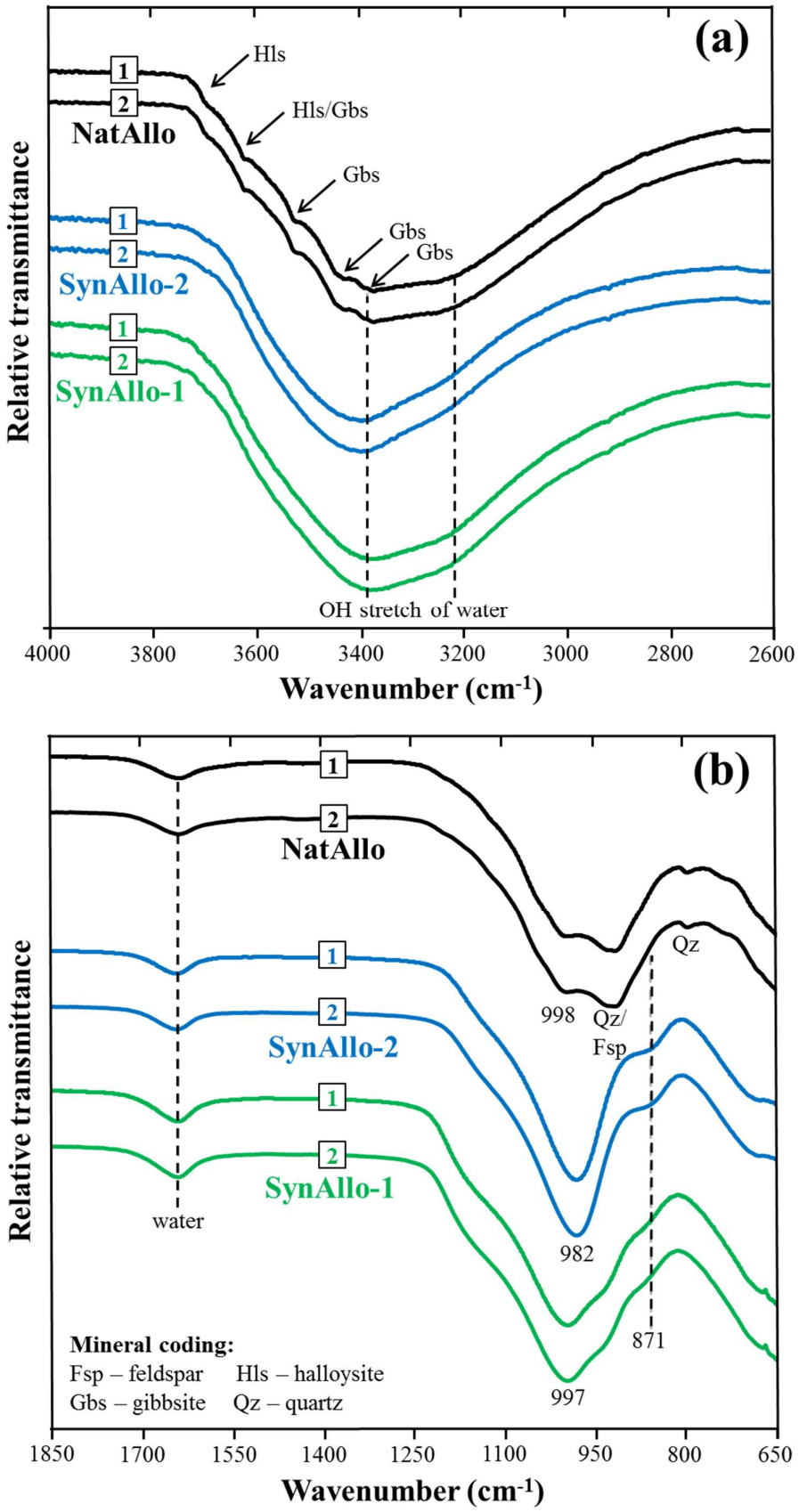

Figure 2. ATR-FTIR spectra of NatAllo, SynAllo-1 and SynAllo-2 before the adsorption experiments (1) and with sorbed Zn^{2+} ions (2). (a) Hydroxyl stretching region; (b) Lattice vibration region.

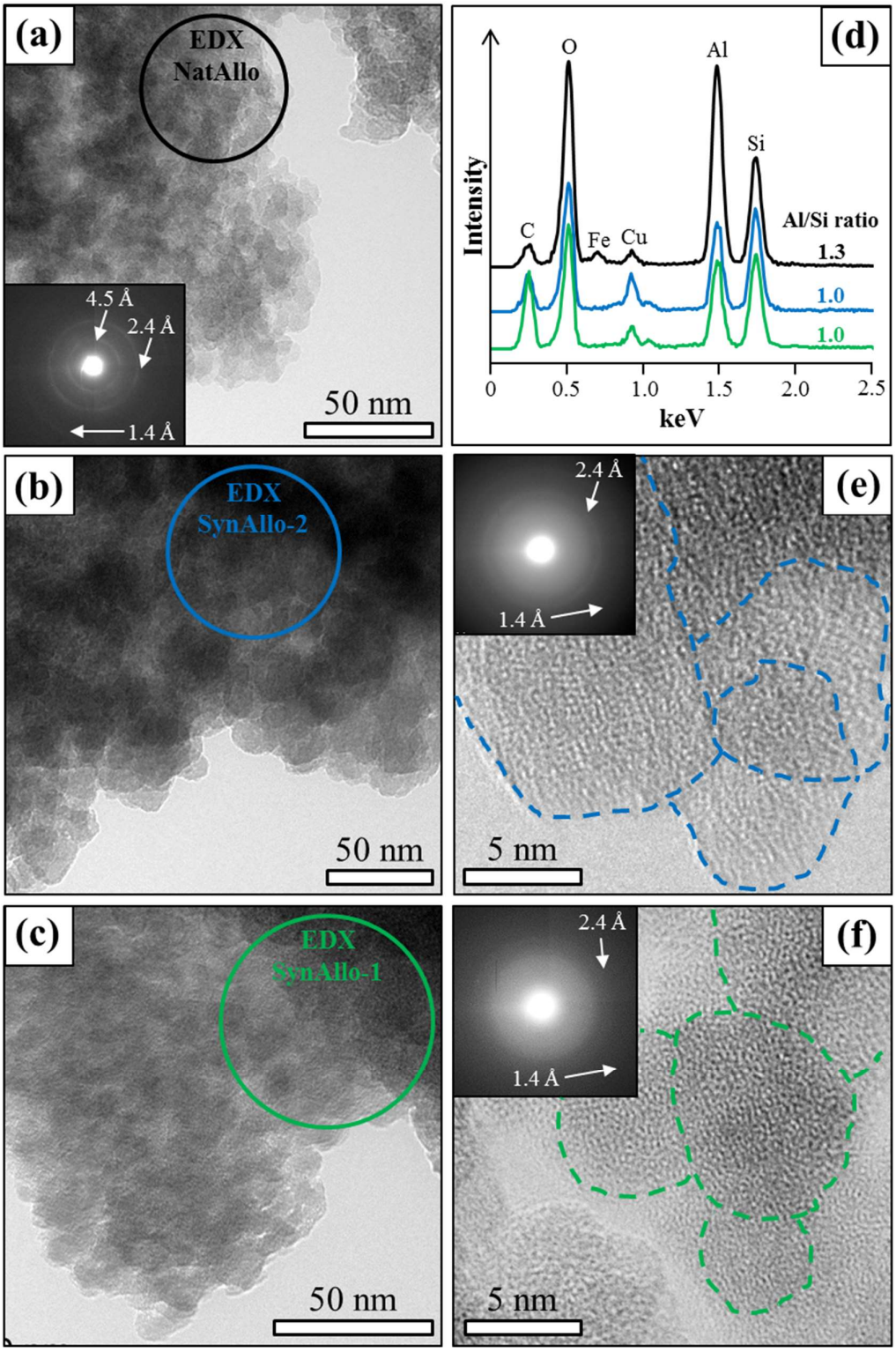

Figure 3. TEM images and SAED patterns of allophane nano-particles used as adsorbents. (a) NatAllo; (b) SynAllo-2; (c) SynAllo-1. (d) TEM-EDX spectra and corresponding averaged atomic Al/Si ratios of natural and synthetic allophanes (spot positions are marked in a–c). The small Fe peak indicates the presence of goethite in NatAllo. (e,f) High-resolution TEM lattice fringe images and related SAED patterns of SynAllo-2 and SynAllo-1, respectively, displaying allophane "nano-ball" structures.

3.3. Structural and chemical characterization of allophane adsorbents

3.3.1. Aqueous speciation of metal ions used as adsorbates

The affinity between a chemical component and the adsorbent controls the extent at which an aqueous metal ion is adsorbed onto a mineral surface. Indeed, the aqueous speciation of a metal ion, pH, contact time, temperature and the metal ion concentration are important factors that determine the kinetics and the efficiency of a given adsorption process [8,12,13,33]. In these experiments, the aqueous speciation of Ba and Sr was predominated by "free" Ba^{2+} and Sr^{2+} ions at pH 8.5 to 4.0. Minor quantities (< 2 %) belonged to $BaCl^{+}$ and $BaOH^{+}$ versus $SrCl^{+}$ and $SrOH^{+}$ aquo-complexes, which indicates that the vast majority of the total Ba and Sr species prevailed in the cationic form. In contrast, the aqueous speciation of Co and Zn was characterized by the sole presence of $HCoO_2^-$ and by the dominance of Zn^{2+}(61 %), $Zn(OH)_2^0$ (19 %), $ZnOH^{+}$ (16 %), $ZnCl^{+}$ (3 %) and $Zn(OH)Cl$ (1 %) aquo-complexes at pH 8.5. At pH ≤ 6.5 for Co and at pH ≤ 7.5 for Zn, however, the Co^{2+} and Zn^{2+} species dominated over trace amounts (< 5 %) of $HCoO_2^-$, $CoCl^{+}$ and $Co(OH)_2^0$ versus $ZnCl^{+}$, $ZnOH^{+}$, $Zn(OH)_2^0$ and $Zn(OH)Cl$ aquo-complexes. From these data it can be inferred that significant changes in the aqueous speciation of Co and Zn did occur in the pH-drift experiments.

All experimental solutions were undersaturated with respect to the least soluble oxyhydroxides of Ba(II), Co(II) and Sr(II) at any time throughout the experiments. However, in the case of aqueous Zn, the experimental solutions were oversaturated with respect to both the $Zn(OH)_2$ polymorphs and $Zn_2(OH)_3Cl$ at pH ≥ 7.3, although none of the latter phases has been detected by XRD and FTIR analyses (Fig. 2).

3.3.2. Effect of contact time on the adsorption kinetics of aqueous metal ions

The effect of contact time on the adsorption behavior of aqueous Ba, Co, Sr and Zn by allophane adsorbents was investigated at pH values of either 8.5 or 5.5 (reflecting the observed minimum and maximum adsorption efficiencies; see section 3.3.3.). It can be inferred from Figure 4 that the metal ion uptake by allophane increased significantly within 3–5 min, but it slowed down afterwards due both to a decrease in the binding sites of the adsorbents and a decrease in the metal ion concentration in solution. More specifically, for aqueous Ba, Sr and Zn, adsorption has been completed within less than 5 min at pH 8.5 (Table 1), while aqueous Co needed 10 min to reach equilibrium. As expected, the removal efficiency strongly decreased and the time to reach adsorption equilibrium increased at decreasing pH (Table 1). This is because the ≡Al-OH° and ≡Si-OH° groups are more protonated under acidic conditions and potential binding sites are less available to retain metal ions [30].

The kinetics of the metal ion uptake by allophane was described by a pseudo-first-order (PFO) model [16,34], according to Eq. 3:

$$ln(q_e - q_t) = -k \cdot t + ln(q_e) \quad (3)$$

where q_e and q_t are the amounts of adsorbate uptake per mass of adsorbent (mg/g) at equilibrium and at time t (min), and k (1/min) is the rate constant of the PFO function. Noteworthy, the plot of Eq. 3 is linear and the calculated and measured q_e values match perfectly (slope: 0.998; n = 24; R^2 = 0.987), which proves the ability of the PFO model to fit the experimental data [16]. The calculated values for *k* and q_e are reported in Table 1.

It can be seen from the kinetic data that metal ion uptake is an exceptionally fast process, which suggests a high affinity of all allophanes to specifically adsorb metal ions. Furthermore, one can see that 5-10 min is enough to achieve adsorption equilibrium under the experimental conditions used in this study, which indicates that physical adsorption rather than ion exchange contributes mainly to the removal of metal ions by natural and synthetic allophane adsorbents. This finding is in line with previous experimental results, where allophane has been successfully used in the remediation of aqueous solutions that were contaminated with, for example, heavy metals cations [15,22,33,35], metal (oxy)anions [18,23,30], heterocyclic organic components [10] and anionic surfactants and organic acids [17,23].

Preprints (www.preprints.org) | NOT PEER-REVIEWED | Posted: 28 June 2018 doi:10.20944/preprints201806.0478.v1

Peer-reviewed version available at Geosciences 2018, 8, 309; doi:10.3390/geosciences8090309

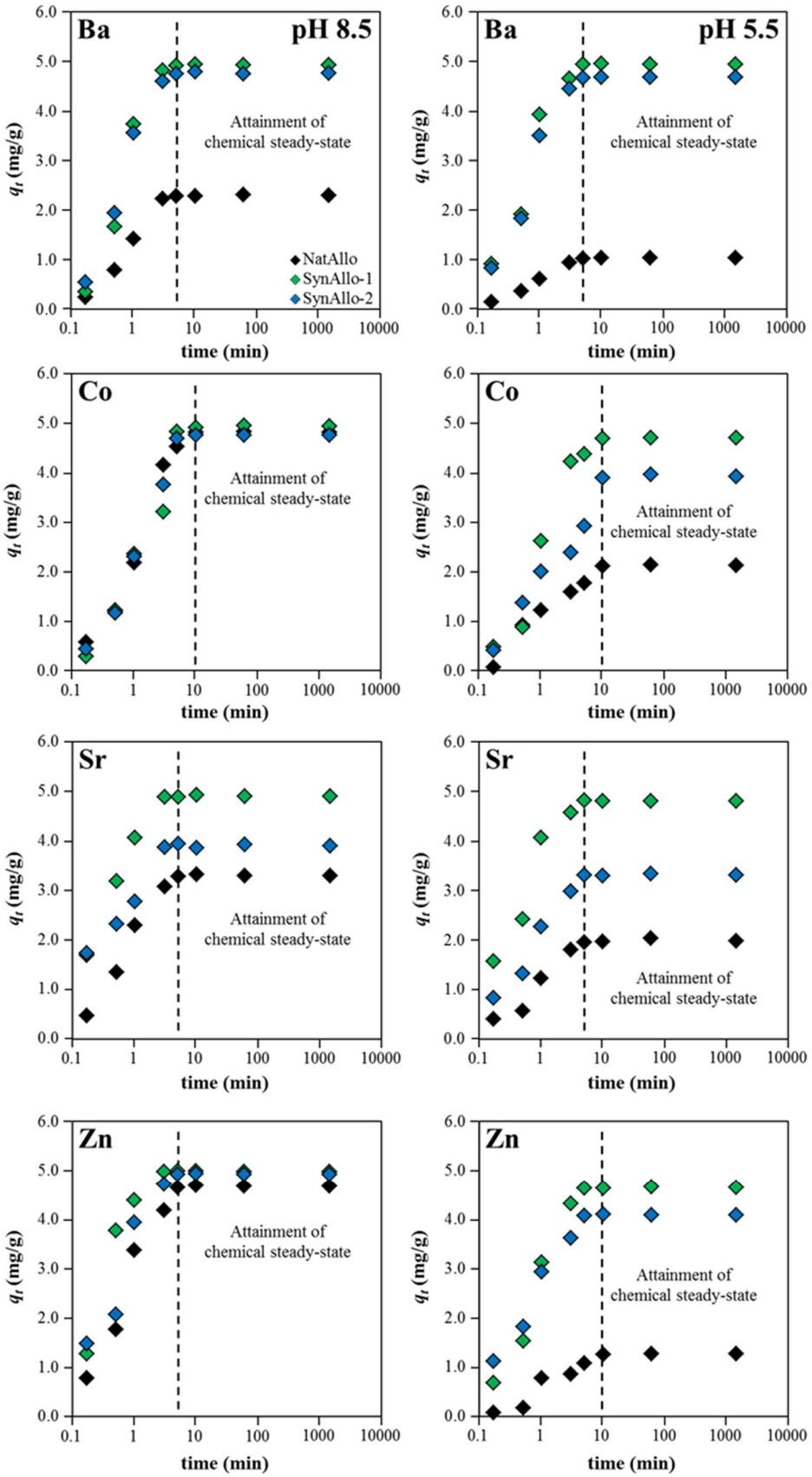

Figure 4. Effect of contact time on the adsorption behavior of aqueous metal ions (initial concentration: 10 mg/L; temperature: 25 °C) by natural and synthetic allophanes at pH 8.5 (left panel) and pH 5.5 (right panel).

Preprints (www.preprints.org) | NOT PEER-REVIEWED | Posted: 28 June 2018 doi:10.20944/preprints201806.0478.v1

Peer-reviewed version available at Geosciences 2018, 8, 309; doi:10.3390/geosciences8090309

Table 1. Comparison of measured ($q_e^{\dagger}$) and calculated ($q_e^{\ddagger}$) adsorption capacities obtained from PFO kinetic model parameters, and compilation of equilibration time (Equil. time) and metal ion removal efficiencies for all allophane adsorbents at pH 8.5 (upper part) and pH 5.5 (lower part).

					Pseudo-first order		
	Adsorbate at pH 8.5	Equil. time (min)	q_e† (mg/g)	Removal rate (%removal)	k (1/min)	q_e (mg/g)	R^2 (-)
NatAllo	Ba^{2+}	5	2.3	45.2	1.090	2.5	0.996
	$[HCoO_2]^-$	10	4.8	95.3	0.573	4.6	0.988
	Sr^{2+}	5	3.3	65.8	0.948	3.1	0.994
	Zn^{2+}	5	4.7	93.5	0.953	4.9	0.953
SynAllo-1	Ba^{2+}	5	4.9	97.1	1.179	4.9	0.992
	$[HCoO_2]^-$	10	4.9	97.6	0.580	4.9	0.942
	Sr^{2+}	3	4.9	97.9	2.003	5.0	0.996
	Zn^{2+}	3	5.0	99.8	2.291	4.9	0.996
SynAllo-2	Ba^{2+}	5	4.8	93.9	1.150	4.8	0.997
	$[HCoO_2]^-$	10	4.8	94.2	0.676	4.8	0.977
	Sr^{2+}	3	3.9	77.9	1.667	3.8	0.978
	Zn^{2+}	5	4.9	98.6	1.271	4.8	0.977

					Pseudo-first order		
	Adsorbate at pH 5.5	Equil. time (min)	q_e† (mg/g)	Removal rate (%removal)	k (1/min)	q_e (mg/g)	R^2 (-)
NatAllo	Ba^{2+}	5	1.0	20.4	0.953	1.1	0.989
	Co^{2+}	10	2.1	42.3	0.475	2.0	0.957
	Sr^{2+}	5	2.0	39.8	0.875	2.0	0.994
	Zn^{2+}	10	1.3	25.4	0.462	1.3	0.965
SynAllo-1	Ba^{2+}	5	5.0	97.4	1.134	4.8	0.971
	Co^{2+}	10	4.7	93.3	0.635	4.6	0.984
	Sr^{2+}	5	4.8	96.4	1.348	4.6	0.942
	Zn^{2+}	5	4.7	93.0	0.986	4.9	0.990
SynAllo-2	Ba^{2+}	5	4.68	92.1	1.162	4.81	0.986
	Co^{2+}	10	3.93	78.0	0.437	4.12	0.925
	Sr^{2+}	5	3.32	66.4	1.046	3.51	0.952
	Zn^{2+}	5	4.09	81.7	1.014	3.98	0.940

3.3.3. Effect of pH on metal ion removal efficiency

Metal ion uptake by allophane depends mainly on pH as acidity affects the aqueous speciation of the metal ions and the (de)protonation degree of the functional ≡Al-OH° and ≡Si-OH° groups at the allophane surface [19,30,35]. Figure 5 presents the evolution of the amounts of aqueous Ba, Co, Sr and Zn adsorbed on allophane from pH 4.0 to 8.5. The corresponding metal ion removal efficiencies at pH 8.5 and pH 4.0 are reported in Table 1. Metal ion uptake by NatAllo was low at pH ≤ 5.0, followed by an adsorbate-dependent increase at pH 5.5 to 7.5 and attained a maximum at pH ≥ 8.0 (Fig. 5). SynAllo-1 revealed the highest removal efficiency (i.e. ≥ 95 %removal) for aqueous Ba at pH 4.0-8.5, Sr at pH 4.5-8.5, Zn at pH 5.5-8.5 and Co at pH 6.0-8.5. SynAllo-2 displayed lower removal efficiencies than SynAllo-1, but it exhibited a good performance at pH ≥ 7.0. NatAllo showed the highest pH-dependency for the metal ion uptake (Fig. 5).

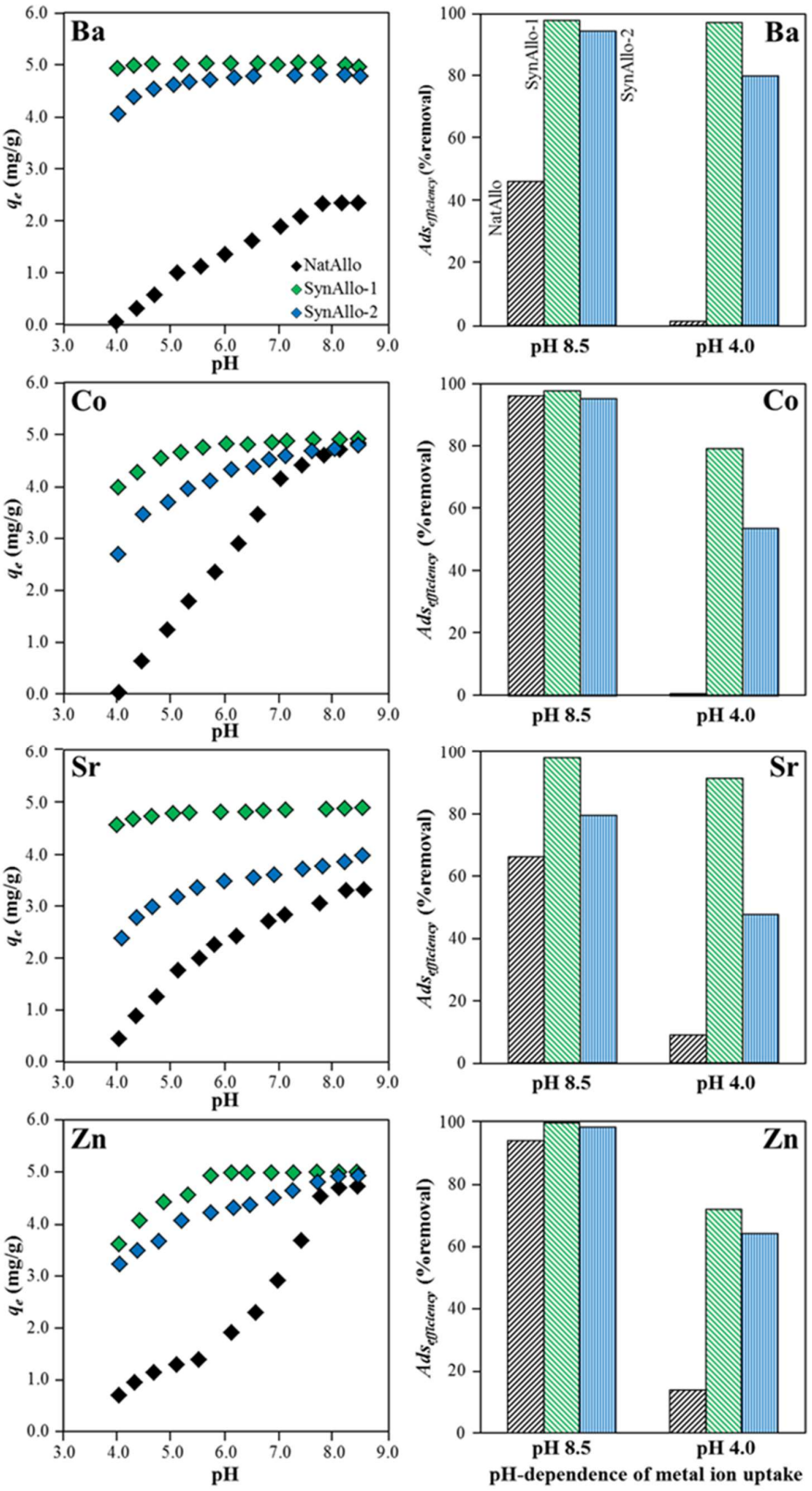

Figure 5. Adsorption of aqueous Ba, Co, Sr and Zn by natural and synthetic allophanes as a function of pH. (left panel) Effect of pH on the adsorption behavior of aqueous metal ions; (right panel) Adsorption efficiencies at pH 8.5 versus pH 4.0.

The obtained results reflect the affinity of the aqueous metal ions to bind to charged allophane surfaces and the tendency to hydrolyze [22]. Si-rich allophane (like SynAllo-1 and SynAllo-2) has a permanent (structural) negative charge, while Al-rich allophane (NatAllo) has a higher amount of variable (pH-dependent) charges [36], which could explain of the pH-depended metal ion uptake of NatAllo, relative to SynAllo-1 and SynAllo-2 (Fig. 5). However, the allophane surface exhibits a positive charge under acidic conditions and thus the metal ion uptake is limited due to repulsive electrostatic forces below the point of zero charge (PZC) value [30]. Thus, net adsorption increases significantly towards alkaline conditions, close to or above the PZC value, which is 7.8 to 9.4 for synthetic allophanes and 5.5 to 6.5 for natural allophanes [21,30,31]. The presence of trace amounts of goethite on the allophane surface could further affect the surface (charge) properties of NatAllo. The small differences in the N_2-BET values (294 to 370 m^2/g) cannot explain the differences observed in the removal efficiencies of NatAllo, SynAllo-1 and SynAllo-2.

3.3.4. Effect of metal ion concentration on the adsorption efficiency

The metal ion concentration plays an important role on controlling the adsorption behavior of allophane. Figure 6 (left panel) shows that the adsorption efficiency increased almost proportionally at higher initial metal ion concentrations, but it slowed down at concentrations higher than 50 mg/L due to the progressive saturation of the binding sites on the allophane surfaces [13]. All allophanes exhibited highly metal ion-specific removal efficiencies. SynAllo-1 revealed a better adsorption for Ba^{2+}, Zn^{2+} and Sr^{2+} than $HCoO_2^-$ ions, while SynAllo-2 showed a preferable uptake of Zn^{2+} over Ba^{2+}, $HCoO_2^-$ and Sr^{2+} ions and NatAllo displayed a better adsorption for Zn^{2+} relative to $HCoO_2^-$, Ba^{2+} and Sr^{2+} ions. The obtained results likely depend on the individual surface charge properties of the adsorbents (although not confirmed by our data) and in particular on the aqueous speciation of the adsorbate [16,33,35,37]. A similar selectivity of metal ion uptake from solution by allophanes grafted with phosphate was observed by Okada et al. [35], which increased in the order $Ni^{2+} \leq Mg^{2+} < Co^{2+} < Ca^{2+} < Zn^{2+} < Cu^{2+}$ at pH 5.1–6.2.

3.3.5. Adsorption isotherms and adsorption mechanism

Figure 6 (right panel) shows the plots of adsorption quantities vs. the metal ion concentrations at equilibrium for the removal of aqueous Ba, Co, Sr and Zn by the allophane absorbents at pH 8.5. The isotherms initially increase sharply at low metal ion concentrations, which suggest that plenty of binding sites are available for adsorption. At higher metal ion concentrations, however, the curves become more flattened, which indicates that no more binding sites at the allophane surfaces are available for further adsorption and that a certain adsorption maximum has been reached. Over the last decades, a huge variety of models have been developed to describe adsorption isotherms, but the most commonly used models are the Langmuir, Freundlich, Dubinin-Radushkevich (D-R model) and Redlich-Peterson models. The advantages, disadvantages and limitations of these models are discussed in detail in the review paper by Tran et al. [16]. In this study, the Langmuir equation and the D-R model are used to describe the isotherms. The linear form of the Langmuir model [38] is defined as Eq. 4:

$$\frac{C_e}{q_e} = \frac{1}{K_L \cdot Q^0_{max}} + \frac{C_e}{Q^0_{max}} \quad (4)$$

where Q^0_{max} denotes the maximum monolayer adsorption capacity of an adsorbent (mg/g) and K_L is the Langmuir adsorption constant (L/mg), which is related to the affinity between the adsorbent and the adsorbate. The values for Q^0_{max} and K_L were computed from the slope and the interception of the linearized plots of C_e/q_e vs. C_e and are reported in Table 2. From these values one can see that the obtained adsorption data are adequately described by the Langmuir model. Following the recommendations of Tran et al. [16] the separation factor R_L (which is sometimes referred to as the equilibrium parameter) has been calculated, according to Eq. 5:

$$R_L = \frac{1}{1 + K_L \cdot C_0} \quad (5)$$

Preprints (www.preprints.org) | NOT PEER-REVIEWED | Posted: 28 June 2018 doi:10.20944/preprints201806.0478.v1

Peer-reviewed version available at Geosciences 2018, 8, 309; doi:10.3390/geosciences8090309

The separation factor is a dimensionless constant, which describes the shape of an isotherm in a given solid-liquid adsorption system. An adsorption process is irreversible at $R_L = 0$, favorable at $0 < R_L < 1$, linear at $R_L = 1$ and unfavorable at $R_L > 1$. The R_L values are shown in Table 2 and indicate that metal ion adsorption by allophane was favorable for all metal ion concentrations.

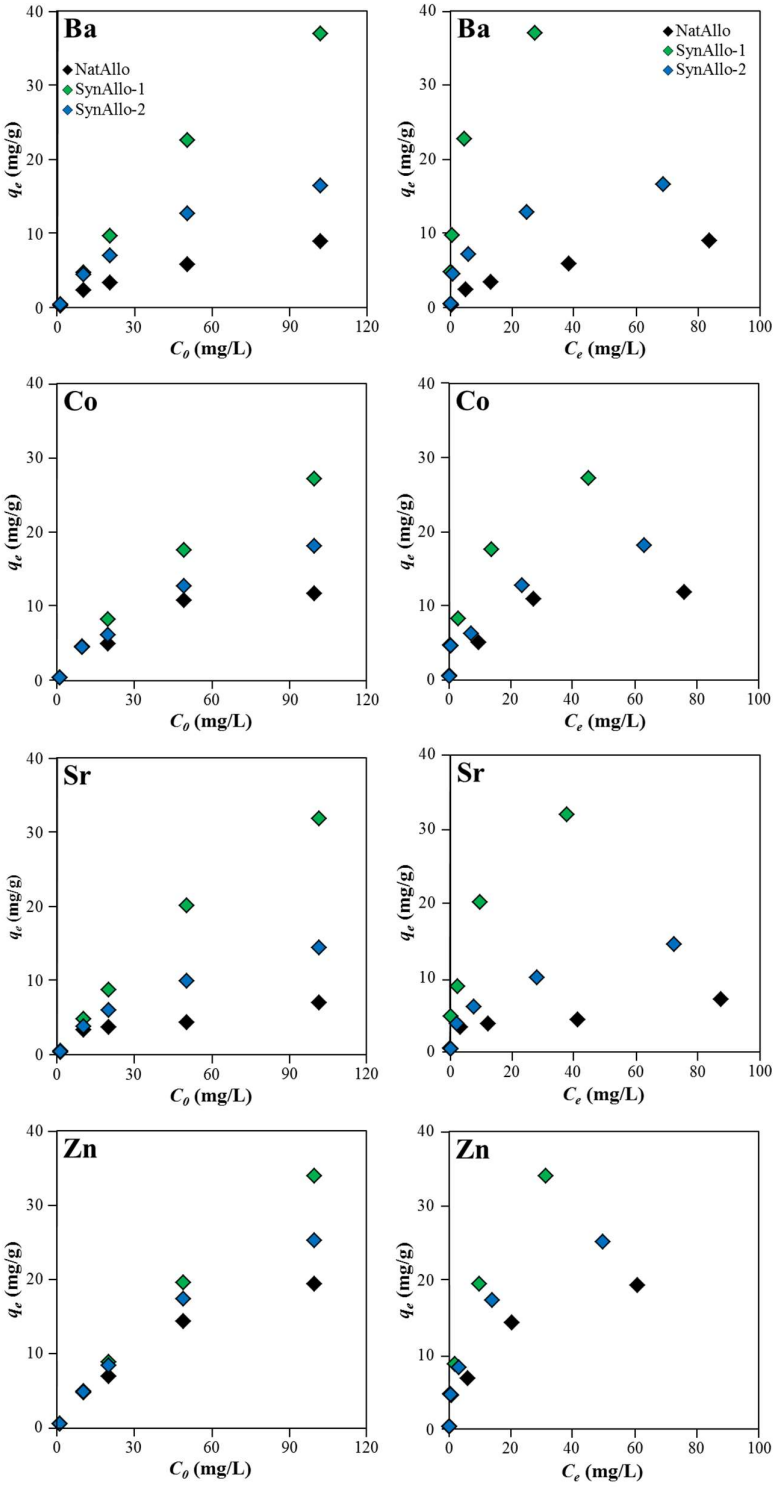

Figure 6. Adsorption behavior of aqueous Ba, Co, Sr and Zn by natural and synthetic allophanes as a function of metal ion concentration. (left panel) Effect of initial metal ion concentration; (right panel) Adsorption isotherms at pH 8.5 and 25 °C.

Preprints (www.preprints.org) | NOT PEER-REVIEWED | Posted: 28 June 2018 doi:10.20944/preprints201806.0478.v1

Peer-reviewed version available at Geosciences 2018, 8, 309; doi:10.3390/geosciences8090309

Table 2. Langmuir isotherm parameters and separation factor (R_L) for the adsorption of aqueous Ba, Co, Sr and Zn on natural and synthetic allophanes.

		Langmuir			
	Adsorbate at pH 8.5	*Q0max* (mg/g)	*KL* (L/mg)	R^2 (-)	*RL* (-)
NatAllo	Ba2+	10.6	0.049	0.947	0.17-0.95
	[HCoO2]-	12.4	0.213	0.974	0.05-0.82
	Sr2+	7.2	0.105	0.927	0.09-0.91
	Zn2+	20.9	0.163	0.971	0.06-0.85
SynAllo-1	Ba2+	38.6	0.676	0.994	0.01-0.60
	[HCoO2]-	29.0	0.226	0.968	0.04-0.81
	Sr2+	34.4	0.265	0.970	0.02-0.58
	Zn2+	36.9	0.240	0.985	0.04-0.80
SynAllo-2	Ba2+	17.2	0.219	0.985	0.04-0.82
	[HCoO2]-	19.3	0.147	0.948	0.06-0.87
	Sr2+	15.9	0.103	0.977	0.09-0.91
	Zn2+	26.9	0.237	0.983	0.04-0.80

The D-R isotherm model has been very often used to describe adsorption phenomena at homogeneous and heterogeneous surfaces. The linear forms of the D-R equation [39] can be written as Eq. 6-7:

$$ln(q_e) = -K_{DR} \cdot \varepsilon^2 + ln(q_{DR}) \quad (6)$$

$$\varepsilon = R \cdot T \cdot ln(1 + \frac{1}{C_e}) \quad (7)$$

where q_{DR} is the maximum monolayer adsorption capacity (mg/g), K_{DR} denotes the D-R model constant (mol^2/kJ^2) related to the mean free energy of adsorption per mole of adsorbate as it migrates to the surface of a given adsorbent from an infinite distance in the aqueous solution, ε is the Polanyi potential (J^2/mol^2), and R and T are the universal gas constant ($8.314 \cdot 10^{-3}$ kJ/(mol·K)) and the absolute temperature (K). The values for q_{DR} and K_{DR} are reported in Table 3. From the activity coefficient K_{DR} the mean free energy of the adsorption process is derived from Eq. 8:

$$E = \frac{1}{\sqrt{2 \cdot K_{DR}}} \quad (8)$$

where E is the free energy change (kJ/mol), which is required to transfer one mole of aqueous metal ions to the adsorbent`s surface. Typical values for E range from 8 to 16 kJ/mol, if the adsorption follows ion exchange, and < 8 kJ/mol, if physical adsorption dominates [13]. The calculated E values are reported in Table 3 and indicate that metal ion uptake by allophane follows physical adsorption rather than chemical ion exchange. However, under the experimental conditions used in this study, the incongruent dissolution of allophane and the subsequent precipitation of secondary Al-(Ba, Co, Sr, Zn)-phases cannot be ruled out, although the aqueous Si and Al concentrations remained at any time below 0.9 and 0.4 mg/L, respectively, which is equivalent to a theoretical dissolution quota of less than 0.3 % for allophane. Nevertheless, for this reason, in the following section we use the term "sorption" to describe metal ion uptake by allophane.

It can be concluded from the shape of the linearized Langmuir and D-R isotherm plots and their correlation coefficients (R^2 values) that our experimental data fit better to the Langmuir model than to the D-R model. Accordingly, the sorption capacity of SynAllo-1 is 38.6 mg/g for Ba^{2+}, 29.0 mg/g for $HCoO_2^-$, 34.4 mg/g for Sr^{2+} and 36.9 mg/g for Zn^{2+}, which is 2 to 3 times higher than the load of

these metal ions on SynAllo-2 and NatAllo. The sorption capacities of some other recently available sorbents for aqueous Ba, Co, Sr and Zn are given in Table 4. It is evident that the sorption capacities of NatAllo, SynAllo-1 and SynAllo-2 for Ba^{2+}, $HCoO_2^-/Co^{2+}$, Sr^{2+} and Zn^{2+} ions are comparable to most other sorbents.

Table 3. Dubinin-Radushkevich parameters and mean free energy change (*E*) for the adsorption of aqueous Ba, Co, Sr and Zn on natural and synthetic allophanes.

		Dubinin-Radushkevich			
	Adsorbate	q_{DR}	K_{DR}	R^2	*E*
	at pH 8.5	(mg/g)	(mol^2/kJ^2)	(-)	(kJ/mol)
NatAllo	Ba^{2+}	7.4	$1.480 \cdot 10^{-8}$	0.979	5.8
	$[HCoO_2]^-$	10.5	$9.115 \cdot 10^{-9}$	0.929	7.4
	Sr^{2+}	6.2	$1.315 \cdot 10^{-8}$	0.962	6.2
	Zn^{2+}	16.3	$1.143 \cdot 10^{-8}$	0.966	6.6
SynAllo-1	Ba^{2+}	44.5	$7.914 \cdot 10^{-9}$	0.996	7.9
	$[HCoO_2]^-$	21.8	$1.008 \cdot 10^{-8}$	0.971	7.0
	Sr^{2+}	26.5	$8.593 \cdot 10^{-9}$	0.977	7.6
	Zn^{2+}	27.4	$1.012 \cdot 10^{-8}$	0.979	7.0
SynAllo-2	Ba^{2+}	15.1	$7.892 \cdot 10^{-9}$	0.988	8.0
	$[HCoO_2]^-$	14.2	$1.009 \cdot 10^{-8}$	0.948	7.0
	Sr^{2+}	12.4	$1.384 \cdot 10^{-8}$	0.990	6.0
	Zn^{2+}	21.2	$1.026 \cdot 10^{-8}$	0.983	7.0

3.4. Application of allophane in water processing technologies

Due to their high affinity to bind aqueous metal cations, natural and synthetic allophanes are good candidate materials for the production of efficient, low cost adsorbents, which could be used for the processing of solutions that are severely contaminated with persistent heavy metals. The high sorption capacity of NatAllo for PO_4^{3-} (37.5 mg/g), AsO_4^{3-} (17.6 mg/g) and F^- (3-5 mg/g) ions has already been proven, rendering this material suitable as an anion absorber [18,36]. The results obtained herein indicate that natural and synthetic allophanes hold a great potential to effectively remove aqueous Ba, Co, Sr and Zn over a wide pH range (Fig. 5, Table 4).

From the application site, it is important to ensure a good performance, a proper workability and a high robustness against modifications in surface charge and electrochemical properties, which could reduce the effectiveness of an adsorbent. Irreversible changes in the allophane properties can be induced during, for example, drying, grinding, heat treatment and phosphate grafting [18,35]. For example, Kaufhold et al. [18] observed a lower F^- sorption capacity for calcined, granulated and dried (at 60 °C) Ecuadorian allophane, compared to naturally moist material. Indeed, drying and heating can cause a decrease of the reactive ≡Al-OH° groups through the formation of ≡Al–O–Al≡ bridges between the allophane primary particles. This process is well-known to affect the surface acidity and decreases the sorption capacity of allophane [40]. Thus, drying of the allophanes could have led to an alteration of their surface (charge) properties, which partly explains the differences observed in their sorption capacities (Table 4). Further tests with allophane suspensions and materials produced by drying have to be done to elucidate the effect of sample pre-treatment on the metal ion removal efficiency of natural and synthetic allophanes.

The evaluation of the adsorption behavior revealed that all allophane adsorbents testes in this study exhibited a performance equal or better than the other available mineral adsorbents such as zeolites, montmorillonite, carbonates and phosphates used for the removal of aqueous Ba, Co, Sr and Zn (Table 4). The XRD, FTIR and TEM data (Figs 1-3) indicate that SynAllo-1 and SynAllo-2

Preprints (www.preprints.org) | NOT PEER-REVIEWED | Posted: 28 June 2018 doi:10.20944/preprints201806.0478.v1

Peer-reviewed version available at Geosciences 2018, 8, 309; doi:10.3390/geosciences8090309

consisted of pure allophane, causing a higher sorption capacity, compared to NatAllo. The sorption capacity of SynAllo-2 was lower than expected, particularly in view of its high allophane content and its highest specific surface area. This indicates that the sorption capacity does not solely depend on the purity of an absorbent and that the specific surface area plays only a minor role. This finding is consistent with previous results [18,22,35], where the sorption efficiency was directly related to the amount of ≡Al-OH° groups in allophane. Herein, it was impossible to quantify the ≡Al-OH° groups due to the presence of halloysite in NatAllo and varying amounts of polymeric SiO_x attached on the octahedral sheet of the synthetic allophanes. In essence, allophane could be applied for remediating wastewater that is contaminated with hazardous metal ions. In order to demonstrate the analogous performance of the allophane adsorbents, further tests regarding the colloidal stability of allophane suspensions and the possibility to regenerate metal ion-loaded allophane have to be performed.

Table 4. Comparison of the adsorption potential of natural and synthetic allophanes with other commercially available adsorbents used for the removal of aqueous Ba, Co, Sr and Zn.

	Adsorbent	Q^0_{max} (mg/g)	Reference
Ba^{2+}	Ca-clinoptilolite	15.3	[37]
	Ca-montmorillonite	15.3	[37]
	Dolomite	4.0	[42]
	Expanded perlite	2.5	[43]
	NatAllo	10.6	This study
	SynAllo-1	38.6	This study
	Syn-Allo-2	17.2	This study
Co^{2+} / $HCoO_2^-$	Al-pillared bentonite clay	38.6	[44]
	Kaolinite	11.0	[45]
	Bentonite/zeolite mixture	2.7	[46]
	Goethite	86.6	[47]
	Lemon peel biosorbent	25.6	[48]
	NatAllo	12.4	This study
	SynAllo-1	29.0	This study
	Syn-Allo-2	19.3	This study
Sr^{2+}	Activated carbon	44.4	[49]
	Almond green hull	116.3	[50]
	Dolomite	1.2	[42]
	Expanded perlite	1.1	[43]
	Polyacrylonitrile-zeolite	98.1	[51]
	NatAllo	7.2	This study
	SynAllo-1	34.4	This study
	Syn-Allo-2	15.9	This study
Zn^{2+}	Activated phosphate rock	12.3	[52]
	Chitosan	290.0	[41]
	Clinoptilolite	12.0	[53]
	Kaolinite	4.9	[54]
	Selenium nanoparticles	60.0	[55]
	NatAllo	20.9	This study
	SynAllo-1	36.9	This study
	Syn-Allo-2	26.9	This study

5. Conclusions

Natural allophane (NatAllo) from Ecuador and synthetic allophanes (SynAllo-1 and SynAllo-2) can be effectively used for the removal of aqueous Ba, Co, Sr and Zn over a wide pH range (e.g. 5.5 ≤ pH ≥ 8.5). Kinetic experiments revealed that the metal ion uptake by allophane reached equilibrium within less than 10 min at 4.0 ≤ pH ≥ 8.5, and can be adequately described by a pseudo-first-order reaction kinetics. The Langmuir model described the adsorption behavior at equilibrium better than the Dubinin-Radushkevich model. The sorption capacity of SynAllo-1 was determined as 38.6 mg/g for Ba^{2+}, 29.0 mg/g for $HCoO_2^-$, 34.4 mg/g for Sr^{2+} and 36.9 mg/g for Zn^{2+} ions at pH 8.5, which is 2 to 3 times higher than for SynAllo-2 and NatAllo. The mean free energy of the adsorption process was calculated to be between 6 and 8 kJ/mol, which indicates that metal ion uptake by allophane is governed by physical adsorption rather than by chemical ion exchange. All allophane adsorbents tested showed sorption capacities comparable to other recently available materials such as zeolites, clay minerals, carbonates and phosphates and could therefore be used for wastewater treatment due to their high adsorption capacity, worldwide occurrence and low cost.

Author Contributions: Conceptualization, Investigation, Visualization, Writing-Original Draft Preparation and Project Administration, A.B.; Experimental, A.B. and A.C.G., Methodology, Data Acquisition and Curation, A.B., A.C.G., C.B., B.P., I.L.-P., S.K. and M.D.; Formal Analysis and Validation, A.B., C.B. and S.K.; Resources, M.D.; Supervision, A.B. and M.D.; Funding Acquisition, A.B. and M.D.

Funding: This research was partly funded by the NAWI Graz Geocentre, Graz University of Technology [F-AF7-221-01].

Acknowledgments: The authors are grateful to M. Hierz and A. Wolf (Graz University of Technology), who assisted us with the synthesis and adsorption experiments. F. Mittermayr (Graz University of Technology) is greatly acknowledged for conducting the BET measurements.

Conflicts of Interest: The authors declare no conflict of interest.

References

[1] Burakov, A.E.; Galunin, E.V.; Burakova, I.V.; Kucherova, A.E.; Agarwal, S.; Tkachev, A.G.; Gupta, V.K. Adsorption of heavy metals on conventional and nanostructured materials for wastewater treatment purposes: A review. *Ecotoxicol. Environ. Saf.* **2018**, *148*, 702-712, 10.1016/j.ecoenv.2017.11.034.

[2] Bhuiyan, M.A.H.; Islam, M.A.; Dampare, S.B.; Parvez, L.; Suzuki, S. Evaluation of hazardous metal pollution in irrigation and drinking water systems in the vicinity of a coal mine area of northwestern Bangladesh. *J. Hazard. Mater.* **2010**, *179*, 1065-1077, 10.1016/j.jhazmat.2010.03.114.

[3] Malik, Q.A.; Khan, M.S. Effect on Human Health due to Drinking Water Contaminated with Heavy Metals. *J. Pollut. Eff. Cont.* **2016**, *5*, No. 1000179, 10.4172/2375-4397.1000179.

[4] Crévecoeur, S.; Debacker, V.; Joaquim-Justo, C.; Gobert, S.; Scippo, M.-L.; Dejonghe, W.; Martin, P.; Thomé, J.-P. Groundwater quality assessment of one former industrial site in Belgium using a TRIAD-like approach. *Environ. Pollut.* **2011**, *159*, 2461-2466, 10.1016/j.envpol.2011.06.026.

[5] Bacquart, T.; Frisbie, S.; Mitchell, E.; Grigg, L.; Cole, C.; Small, C.; Sarkar, B. Multiple inorganic toxic substances contaminating the groundwater of Myingyan Township, Myanmar: arsenic, manganese, fluoride, iron, and uranium. *Sci. Total. Environ.* **2015**, *517*, 232-245, 10.1016/j.scitotenv.2015.02.038.

[6] Chabukdhara, M.; Gupta, S.K.; Kotecha, Y.; Nema, A.K. Groundwater quality in Ghaziabad district, Uttar Pradesh, India: Multivariate and health risk assessment. *Chemosphere* **2017**, *179*, 167-178, 10.1016/j.chemosphere.2017.03.086.

[7] Calzadilla, A.; Rehdanz, K.; Tol, R.S.J. Water scarcity and the impact of improved irrigation management: a computable general equilibrium analysis. *Agric. Econ.* **2011**, *42*, 305-323, 10.1111/j.1574-0862.2010.00516.x.

[8] Fu, F.; Wang, Q. Removal of heavy metal ions from wastewaters: A review. *J. Environ. Manage.* **2011**, *92*, 407-418, 10.1016/j.jenvman.2010.11.011.

[9] Carolin, C.F.; Kumar, P.S.; Saravanan, A.; Joshiba, G.J.; Naushad, M. Efficient techniques for the removal of toxic heavy metals from aquatic environment: A review. *J. Environ. Chem. Eng.* **2017**, *5*, 2782-2799, 10.1016/j.jece.2017.05.029.

[10] Iyoda, F.; Hayashi, S.; Arakawa, S.; John, B.; Okamoto, M.; Hayashi, H.; Yuan, G. Synthesis and adsorption characteristics of hollow spherical allophane nano-particles. *Appl. Clay Sci.* **2012**, *56*, 77-83, 10.1016/j.clay.2011.11.025.

[11] Yuan, G.; Wada, S.I. Allophane and imogolite nanoparticles in soil and their environmental applications. In *Nature's Nanostructures*; Barnard, A.S., Guo, H.B., Eds.; Pan Stanford Publishing Pte Ltd, 2012; pp. 485-508, 9789814316828.

[12] Babel, S.; Kurniawan, T.A. Low-cost adsorbents for heavy metals uptake from contaminated water: a review. *J. Hazard. Mater.* **2003**, *B97*, 219-243. 10.1016/S0304-3894(02)00263-7.

[13] Singha, A.S.; Guleria, A. Chemical modification of cellulosic biopolymer and its use in removal of heavy metal ions from wastewater. Int. J. Biol. Macromol. 2014, 67, 409-417, 10.1016/j.ijbiomac.2014.03.046.

[14] Ismadji, S.; Soetaredjo, F.E.; Ayucitra, A. Natural Clay Minerals as Environmental Cleaning Agents. In *Clay Materials for Environmental Remediation*; Ismadji, S., Soetaredjo, F.E., Ayucitra, A., Eds.; SpringerBriefs in Green Chemistry for Sustainability, Springer Nature, 2015, pp. 5–37, 978-3-319-16711-4.

[15] Mukai, H.; Hirose, A.; Motai, S.; Kikuchi, R.; Tanoi, K.; Nakanishi, T.M.; Yaita, T.; Kogure, T. Cesium adsorption/desorption behavior of clay minerals considering actual contamination conditions in Fukushima. *Sci. Rep.* **2016**, *6*, No. 21543, 10.1038/srep21543.

[16] Tran, H.N.; You, S.-J.; Hosseini-Bandegharaei, A.; Chao, H.-P. Mistakes and inconsistencies regarding adsorption of contaminants from aqueous solutions: A critical review. *Wat. Res.* **2017**, *120*, 88-116, 10.1016/j.watres.2017.04.014.

[17] Nishikiori, H.; Kobayashi, K.; Kubota, S.; Tanaka, N.; Fujii, T. Removal of detergents and fats from waste water using allophane. *Appl. Clay Sci.* **2010**, *47*, 325-329, 10.1016/j.clay.2009.11.040.

[18] Kaufhold, S.; Dohrmann, R.; Abidin, Z.; Henmi, T.; Matsue, N.; Eichinger, L.; Kaufhold, A.; Jahn, R. Allophane compared with other sorbent minerals for the removal of fluoride from water with particular focus on a mineable Ecuadorian allophane. *Appl. Clay Sci.* **2015**, *5*, 25-33, 10.1016/j.clay.2010.06.018.

[19] Parfitt, R.L. Allophane in New Zealand – a review. *Aust. J. Soil Res.* **1990**, *28*, 343-360, 10.1071/SR9900343.

[20] Hashizume, H. Adsorption of nucleic acid bases, ribose, and phosphate by some clay minerals. *Life* **2015**, *5*, 637-650, 10.3390/life5010637.

[21] Wu, Y.; Lee, C.-P.; Mimura, H.; Zhang, X.; Wei, Y. Stable solidification of silica-based ammonium molybdophosphate by allophane: Application to treatment of radioactive cesium in secondary solid wastes generated from fukushima. *J. Hazard. Mater.* **2018**, *341*, 46-54, 0.1016/j.jhazmat.2017.07.044.

[22] Clark, C.J.; McBride, M.B. Chemisorption of Cu(II) and Co(II) on allophane and imogolite. *Clays Clay Miner.* **1984**, *32*, 300-310, 10.1346/CCMN.1984.0320408.

[23] Jara, A.A.; Violante, A.; Pigna, M.; Mora, M.L. Mutual interactions of sulfate, oxalate, citrate, and phosphate on synthetic and natural allophanes. *Soil Sci. Soc. Am. J.* **2006**, *70*, 337-346, 10.2136/sssaj2005.0080.

[24] Kaufhold, S.; Kaufhold, A.; Jahn, R.; Brito, S.; Dohrmann, R.; Hoffmann, R.; Gliemann, H.; Weidler, P.; Frechen, M. A new massive deposit of allophane raw material from Ecuador. *Clays Clay Miner.* **2009**, *57*, 72-81, 10.1346/CCMN.2009.0570107.

[25] Wada, S.-I.; Eto, A.; Wada, K. Synthetic allophane and imogolite. *J. Soil Sci.* **1979**, *30*, 347-355, 10.1111/j.1365-2389.1979.tb00991.x.

[26] Baldermann, A.; Dohrmann, R.; Kaufhold, S.; Nickel, C.; Letofsky-Papst, I.; Dietzel, M. The Fe-Mg-saponite solid solution series – a hydrothermal synthesis study. *Clay Miner.* **2014**, *49*, 391-415, 10.1180/claymin.2014.049.3.04.

[27] Baldermann, A.; Warr, L.N.; Letofsky-Papst, I.; Mavromatis, V. Substantial iron sequestration during green-clay authigenesis in modern deep-sea sediments. *Nat. Geosci.* **2015**, *8*, 885-889, 10.1038/NGEO2542.

[28] Baldermann, A.; Dietzel, M.; Mavromatis, V.; Mittermayr, F.; Warr, L.N.; Wemmer, K. The role of Fe on the formation and diagenesis of interstratified glauconite-smectite and illite-smectite: A case study of Upper Cretaceous shallow-water carbonates. *Chem. Geol.* **2017**, *453*, 21-34, 10.1016/j.chemgeo.2017.02.008.

[29] Kaufhold, S.; Ufer, K.; Kaufhold, A.; Stucki, J.W.; Anastácio, A.S.; Jahn, R.; Dohrmann, R. Quantification of allophane from Ecuador. *Clays Clay Miner.* **2010**, *58*, 707-716, 10.1346/CCMN.2010.0580509.

[30] Opiso, E.; Sato, T.; Yoneda, T. Adsorption and co-precipitation behavior of arsenate, chromate, selenate and boric acid with synthetic allophane-like materials. *J. Hazard. Mater.* **2009**, *170*, 79-86, 10.1016/j.jhazmat.2009.05.001.

[31] Levard, C.; Doelsch, E.; Basile-Doelsch, I.; Abidin, Z.; Miche, H.; Masion, A.; Rose, J.; Borschneck, D.; Bottero, J.-Y. Structure and distribution of allophanes, imogolite and proto-imogolite in volcanic soils. *Geoderma* **2012**, *183-184*, 100-108, 10.1016/j.geoderma.2012.03.015.

[32] Baldermann, A.; Mavromatis, V.; Frick, P.M.; Dietzel, M. Effect of aqueous Si/Mg ratio and pH on the nucleation and growth of sepiolite at 25 °C. *Geochim. Cosmochim. Acta* **2018**, *227*, 211-226, 0.1016/j.gca.2018.02.027.

[33] Usiyama, T.; Fukushi, K. Predictive model for Pb(II) adsorption on soil minerals (oxides and low-crystalline aluminum silicate) consistent with spectroscopic evidence. *Geochim. Cosmochim. Acta* **2016**, *190*, 134-155, 10.1016/j.gca.2016.06.022.

[34] Lagergren, S. Zur theorie der sogenannten adsorption geloster stoffe. *K. Sven.Vetenskapsakad. Handl.* **1898**, *24*, 1-39.

[35] Okada, K.; Nishimuta, K.; Kameshima, Y.; Nakajima, A. Effect on uptake of heavy metal ions by phosphate grafting of allophane. *J. Colloid Interface Sci.* **2005**, *286*, 447-454, 10.1016/j.jcis.2005.01.033.

[36] Kaufhold, A. *Eigenschaften von Allophan aus Ecuador (Santo Domingo de los Colorados) und Anwendungspotential als Rohstoff*, Hallenser Bodenwissenschaftliche Abhandlungen 16, Germany, 2011; pp. 1–175, 978-3-86247-172-0.

[37] Chávez, M.L.; de Pablo, L.; García, T.A. Adsorption of Ba^{2+} by Ca-exchange clinoptilolite tuff and montmorillonite clay. *J. Hazard. Mater.* **2010**, *175*, 216-223, 10.1016/j.jhazmat.2009.09.151.

[38] Langmuir, I. The adsorption of gases on plane surfaces of glass, mica and platinum. *J. Am. Chem. Soc.* **1918**, *40*, 1361-1403, 10.1021/ja02242a004.

[39] Dubinin, M.M.; Radushkevich, L.V. Equation of the characteristic curve of activated charcoal. *Proc. Acad. Sci. USSR Phys. Chem. Sect.* **1947**, *55*, 331-333.

[40] Khan, H. Water Adsorption and Surface Acidity of Nano-Ball Allophane as Affected by Heat Treatment. *J. Environ. Sci. Technol.* **2009**, *2*, 22-30, 10.3923/jest.2009.22.30.

[41] Kyzas, G.Z.; Siafaka, P.I.; Pavlidou, E.G.; Chrissafis, K.J.; Bikiaris, D.N. Synthesis and adsorption application of succinyl-grafted chitosan for the simultaneous removal of zinc and cationic dye from binary hazardous mixtures. *Chem. Eng. J.* **2015**, *259*, 438-448, 10.1016/j.cej.2014.08.019.

[42] Ghaemi, A.; Torab-Mostaedi, M.; Ghannadi-Maragheh, M. Characterizations of strontium(II) and barium(II) adsorption from aqueous solutions using dolomite powder. *J. Hazard. Mater.* **2011**, *190*, 916-921, 10.1016/j.jhazmat.2011.04.006.

[43] Torab-Mostaedi, M.; Ghaemi, A.; Ghassabzadeh, H.; Ghannadi-Maragheh, M. Removal of strontium and barium from aqueous solutions by adsorption onto expanded Perlite. *Can. J Chem. Eng.* **2011**, *89*, 1247-1254, 10.1002/cjce.20486.

[44] Manohar, D.M.; Noeline, B.F.; Anirudhan, T.S. Adsorption performance of Al-pillared bentonite clay for the removal of cobalt(II) from aqueous phase. *Appl. Clay Sci.* **2006**, *31*, 194-206, 10.1016/j.clay.2005.08.008.

[45] Bhattacharyya, K.G.; Gupta, S.S. Kaolinite and montmorillonite as adsorbents for Fe(III), Co(II) and Ni(II) in aqueous medium. *Appl. Clay Sci.* **2008**, *41*, 1-9, 10.1016/j.clay.2007.09.005.

[46] Al-Dwairi, R.A.; Al-Rawajfeh, A.E. Removal of cobalt and nickel from wastewater by using Jordan low-cost zeolite and bentonite. *J. Univ. Chem. Technol. Metall.* **2012**, *47*, 69-76.

[47] Mohapatra, M.; Mohapatra, L.; Singh, S.; Anand, S.; Mishra, B.K. A comparative study on Pb(II), Cd(II), Cu(II), Co(II) adsorption from single and binary aqueous solutions on additive assisted nano-structured goethite. *Int. J. Eng. Sci. Technol.* **2010**, *2*, 89-103, 10.4314/ijest.v2i8.63784

[48] Bhatnagara, A.; Minocha, A.K.; Sillanpää, M. Adsorptive removal of cobalt from aqueous solution by utilizing lemon peel as biosorbent. *Biochem. Eng. J.* **2010**, *48*, 181-186, 10.1016/j.bej.2009.10.005.

[49] Chegrouche, S.; Mellah, A.; Barkat, M. Removal of strontium from aqueous solutions by adsorption onto activated carbon: kinetic and thermodynamic studies. *Desalination* **2009**, *235*, 306-318, 10.1016/j.desal.2008.01.018.

[50] Ahmadpour, A.; Zabihi, M.; Tahmasbi, M.; Rohani Bastami, T. Effect of adsorbents and chemical treatments on the removal of strontium from aqueous solutions. *J. Hazard. Mater.* **2010**, *182*, 552-556, 10.1016/j.jhazmat.2010.06.067.

[51] Faghihian, H.; Iravani, M.; Moayed, M.; Ghannadi-Maragheh, M. A novel polyacrylonitrile–zeolite nanocomposite to clean Cs and Sr from radioactive waste. *Environ. Chem. Lett.* **2013**, *11*, 277-282, 10.1007/s10311-013-0399-1.

[52] Elouear, Z.; Bouzid, J.; Boujelben, N.; Feki, M.; Jamoussi, F.; Montiel, A. Heavy metal removal from aqueous solutions by activated phosphate rock. *J. Hazard. Mater.* **2008**, *156*, 412-420, 10.1016/j.jhazmat.2007.12.036.

[53] Stojakovic, D.; Hrenovic, J.; Mazaj, M.; Rajic, N. On the zinc sorption by the Serbian natural clinoptilolite and the disinfecting ability and phosphate affinity of the exhausted sorbent. *J. Hazard. Mater.* **2011**, *185*, 408-415, 10.1016/j.jhazmat.2010.09.048.

[54] Shahmohammadi-Kalalagh, S.; Babazadeh, H.; Nazemi, A.H.; Manshouri, M. Isotherm and kinetic studies on adsorption of Pb, Zn and Cu by kaolinite. *Caspian J. Environ. Sci.* **2011**, *9*, 243-255.

[55] Jain, R.; Jordan, N.; Schild, D.; van Hullebusch, E.D.; Weiss, S.; Franzen, C.; Farges, F.; Hübner, R.; Lens, P.N.L. Adsorption of zinc by biogenic elemental selenium nanoparticles. *Chem. Eng. J.* **2015**, *260*, 855-863, 10.1016/j.cej.2014.09.057.